Valley and Bedform-Scale Ground and Surface Water Interaction and its Potential for Thermal Refuge in a Restored Reach

A Thesis

Presented in Partial Fulfillment of the Requirements for the

Degree of Master of Science

with a

Major in Geological Engineering

in the

College of Graduate Studies

University of Idaho

by

Jordan Frye

Approved by:

Major Professor: Andy Tranmer, Ph.D.

Committee Members: Daniele Tonina, Ph.D.; Caroline Ubing, M.S.

Department Administrator: Fritz Fiedler Ph.D.

August 2023

Abstract

Water temperature is a controlling variable that influences fish passage and migration, regulates the metabolic processes of organisms in the channel and substrate, and ultimately controls the distribution and quality of available habitat for a range of aquatic species. Anthropogenic activities and climate change have impacted stream water temperatures; therefore, the formation and restoration of thermal refuge, areas with temperature differences greater than 0.5 °C relative to average channel temperature and within the biologically required temperature range, are becoming management and restoration priorities. Currently, there is no consensus on which morphologic features (e.g., pools, riffles, alcoves, bars, and spring-fed spring channels) provide the most effective thermal refuge. Here we evaluate the effectiveness of various constructed morphologic features at creating thermal refuge over 2.5 km reach of a recently restored gravel-bed river. Wells monitored valley groundwater levels and hyporheic flux probes in the streambed quantified the direction and magnitude of hyporheic flows. In addition, a longitudinal survey was performed during summer low-flow conditions to measure water temperature and water surface elevation profiles.

Results show that valley-scale groundwater-surface water gaining and losing pattern overwhelmed hyporheic exchange induced by fluvial morphologic features, e.g., pool-riffle such that their median hyporheic flux constitutes less than 0.03% of the in-stream summer low flow discharge. While hyporheic flux magnitudes were similar in pools, the accumulation of cool hyporheic flow in the low-velocity section of the pool and increased thermal buffering from solar radiation can provide thermal refuge of 0.5 °C. Secondary spring channels derived from hyporheic flows provided cool water temperatures of 13 °C, but due to low velocities and lack of shade, the water temperature rose above the stress threshold to 18 °C before it entered the river.. Constructed alcoves, riffles, and bars generated little observed thermal refuge in the study reach. Results outline the conditions of various morphologic features in generating thermal refuge that may be used to help guide future restoration projects.

Acknowledgments

Firstly, I would like to acknowledge my major Professor Andy Tranmer, he has been an incredible mentor who has supported and encouraged me the last 3 years, especially when things weren't going well. Thank you for your time, knowledge, patience, and understanding throughout this journey, I am incredibly grateful for your help and would not have been able to do it without you. I would also like to thank my committee members Daniele Tonina and Caroline Ubing for their time and expertise. I would also like to thank PhD student Andrea Bertagnoli for his assistance during this process. I would also like to thank the entire Center for Ecohydraulics family for welcoming me from the moment I enrolled.

Dedication

I would like to thank my family and friends for their support through this process. My parents Pauline and Deron Frye have made countless sacrifices since I was born to put me in the position I am in today. They have shown me unconditional love and support and am incredibly grateful to have them as parents, their sacrifices do not go unnoticed. To my sister Morgan who has been my biggest fan, I would not be here if it wasn't for you, your accomplishments in school and softball inspire me to be better every day. Lastly, I would like to thank my friends Casey Sanders, Joey Greco, Chase Young, and Grace Fallar for your continued support.

Table of Contents

Abstract ii

Acknowledgments iii

Dedication iv

Table of Contents v

List of Tables vii

List of Figures viii

Chapter 1 1

1. Introduction 1

2. Methods 3

2.1 Study Area 3

2.2 River Restoration Approach 3

2.3 Measurements and techniques 4

3. Results 7

3.1 Valley-scale features driving hyporheic and thermal conditions 7

3.2 Unit-scale features driving hyporheic and thermal conditions 9

3.3 Geomorphic features maintaining thermal refuge 10

4. Discussion 11

4.1 Valley-scale hyporheic and thermal conditions 11

4.2 Performance of valley-scale and unit-scale morphologic units to induce hyporheic flow 12

4.3 Identification of Thermal Refuge 14

5. Conclusion 17

References 18

Figures and Tables 26

Appendix A 33

Figure A1: GPS Unit Set up for Thermal Survey and Hyporheic Flux Probe Construction 33

Figure A2: Valley Scale GW-SW Analysis Methodology 34

Figure A3: Mechanisms maintaining cool pool temperatures 35

Figure A4: Fluxes of all probes 36

Figure A5: Fish Snorkel Survey 37

List of Tables

Table 1: Can Unit-scale Features Overwhelm Groundwater Gradients 32

List of Figures

Figure 1: Site Area 26
Figure 2: Water Temperatures for 2021 Water Year + GW Levels and Stage 27
Figure 3: Valley Scale GW-SW Analysis With Discharge Measurement 28
Figure 4: Box Plots for Each Morphology 29
Figure 5: Spring Channels 30
Figure 6: Temperatures at Exit of Backfilled Channel 31

Chapter 1

1. Introduction

Water temperature is a controlling variable that mediates the physical and geochemical properties in the water column, fish passage, and the distribution of available habitat for aquatic species (e.g., Ebersole et al., 2001; Tranmer et al., 2018; 2020; Keefer et al., 2020; Sullivan et al., 2021). As global warming continues to raise temperatures in fluvial environments, habitat for cold-water fish will experience a significant reduction of thermally suitable habitat (e.g., Bilby, 1984; Eaton and Scheller, 1996; Isaak et al., 2016; Spanjer et al 2022; Reeder et al., 2021). During the summer months, when water temperatures exceed species-specific temperature thresholds, cold-water areas within the channel can potentially provide thermal refuge (e.g., Kurylyk et al., 2014; Ritter et al., 2020). Thermal refuges are spatially discrete areas that are thermally distinct from the mean water temperature in the river by ≥0.5° C and are below species specific stress thresholds (e.g., Dugdale et al., 2013; Fakhari et al., 2022; Sullivan et al., 2021). Cold-water refuges in rivers and streams can play significant physiological and ecological roles during warm summer months because water temperature is the driving factor that determines metabolic rates of fish and other aquatic organisms on which they feed (e.g., Benjamin et al., 2020; Torgerson et al., 2012; Vinson et al., 2001; Tranmer et al., 2018). Fish are capable of detecting differences in temperature of 0.1° C and have been observed to move to thermally favorable areas when temperature variations are present (e.g., Benjamin et al., 2020; Favrot et al., 2018; Torgerson et al., 2012). When water temperatures approach stressful thermal thresholds, fish engage in thermoregulatory behavior, movement by an organism to occupy more favorable thermal environments, to mitigate physiological stress (e.g., Bilby, 1984; Weigel et al., 2017). Cold-water species can use a thermal refuge to lower their body temperature, reduce metabolic energy costs, and exploit resources in unfavorable environments (e.g., Westhoff et al., 2016).

Identifying areas of thermal refuge is challenging as they change both spatially and temporally over the year. Numerous methods have been used to identify the presence and spatial distribution of thermal refuges in fluvial environments during high-temperature conditions. At a watershed scale, the spatial distribution of thermal refuges can be estimated using GIS models that consider landscape variables such as valley width and slope, land use types, and vegetation characteristics (Monk et al., 2013). These watershed-scale approaches can provide a preliminary analysis on potential restoration reaches within a watershed, but these first-order estimates are unable to identify the specific locations of thermal refuge within a reach. More spatially refined methodologies have been used to identify thermal refuge at the reach scale using aerial thermal infrared surveys (Dugdale et al., 2016;

Torgersen et al., 2001), three-dimensional arrays of in-situ temperature loggers (Greer et al., 2019), fiber optic distributed temperature sensing (Read et al., 2013), handheld digital thermometers (Ebersole et al., 2003), or a combination of these methods. These methods can provide valuable data but suffer from sensitivity to shading or reflection, high costs, and low spatial resolution. Therefore, a new approach is needed to rapidly collect water temperature data at larger spatial scales that is both spatially accurate and cost effective to identify thermal refuges within a reach.

Thermal refuge typically forms as a patch or plume when different flow patterns with unique distinct temperatures converge or water of different temperatures become vertically layered (Sullivan et al., 2021). Groundwater temperature is relatively insensitive to short-term air temperature changes and diel warming; therefore, groundwater seeps and other areas with strong groundwater interaction have high potential for generating thermal refuge (e.g., Constantz, 1998; Guenther et al., 2014; Hayashi and Rosenberry, 2002). Earlier studies have identified morphologic features that can create thermal refuge, such as cold-water tributaries discharging into streams, shaded areas, deep-water pools, cold alcoves, or streambed hyporheic flow (e.g., Bilby, 1984; Merriam and Petty, 2018; Torgerson et al., 2012). However, few studies have compared and quantified which morphologic features are most effective at generating and maintaining thermal refuge.

River restoration projects typically aim to generate hydraulic and thermal processes that improve habitat quality and distribution (e.g., Beechie et al., 2010; Tranmer et al., 2022; Wohl et al., 2015). To address increasing water temperatures for migratory and resident aquatic species, many restoration activities are constructing geomorphic features that can increase hyporheic exchange and thermal heterogeneity in the channel (e.g., Beechie et al., 2013; Gariglio et al., 2013; Singh et al., 2018; Tonina and Buffington, 2007). Restoration of thermal heterogeneity and refuges through coupled river-floodplain systems generally relies on the identification of existing thermal anomalies within the river corridor that can be incorporated into restoration design and implementation (e.g., Kurylyk et al., 2014; Torgerson et al., 2012). Various restoration methods have been proposed to enhance existing thermal refuges and/or create new ones by increasing hyporheic exchange (e.g., Boano et al, 2008; Poole et al., 2006; Sawyer and Cardenas, 2012). Active restoration methods typically involve the installation of instream wood/rock structures and the excavation of primary and secondary channels to promote hyporheic exchange with groundwater (e.g., Bakke et al., 2020; Goniea et al., 2006; Kurylyk et al., 2014). Hyporheic flow occurs in the lateral, longitudinal, and vertical directions, making it difficult to quantify the boundaries, and how flow paths and residence times might change if boundary conditions are altered. Therefore, restoration methods that install instream structures and excavate new channels can provide unpredictable results regarding the creation of thermal refuge

(e.g., Boano et al, 2008; Theodoropoulos et al., 2020). Thus, there is still uncertainty in which restored features reliably create thermal refuge from enhanced hyporheic exchange. Here we study various constructed morphologic features during restoration and asses their effectiveness at creating and maintaining thermal refuge for cold-water salmonids using a combination of methods that includes hyporheic flux probes, a valley-scale groundwater analysis, and a new low-cost thermal survey method to identify the distribution and spatial extent of local water temperatures.

2. Methods

2.1 Study Area

The study site is located in a recently restored 2.5 km-long reach on the Grande Ronde River (GRR), a tributary to the Lower Snake River near La Grande, Oregon (Fig. 1). The valley slope is 0.59% and average valley width is 650 m. The semi-confined gravel-bed reach has a pool-riffle morphology, with an average channel width of 20 m, a slope of 0.38%, and a median grain size of 45 mm. Average daily summer high air temperatures are approximately 30 °C and average daily winter low temperatures are typically -4 °C. The GRR is a snowmelt-dominated system with peak flows (~56 m^3/s) occurring in April and May while low-flow conditions (~0.35 m^3/s) exist from July through October. The basin is 73% forested and the surrounding bedrock is primarily basaltic igneous rock with some marine sedimentary and metamorphic rock (USBR, 2016). Geotechnical analysis shows that the bedrock begins 10-15 meters below the ground surface and is overlain by permeable sand and gravel layers that extend upwards to a thin layer of topsoil and some clay lenses (Legg and Ybarrondo, 2015). Riparian vegetation consists primarily of Ponderosa pine (*Pinus ponderosa*), Black cottonwood (*Populus trichocarpa*), Snowberry (*Symphoricarpos albus*), and mixed willows (*Salix spp.*), but is sparse in the reach and provides limited shade along the channel.

2.2 River Restoration Approach

The historic channel was straightened in the 1800s to facilitate splash-dam logging (USBR, 2016), which created a wide, shallow-bed channel (USBR 2018). The pre-restoration reach was considered thermally stressful for Chinook salmon during summer months, which allowed for little rearing habitat and created a thermal barrier for spawning activities in the upper catchment (USBR, 2016). Chinook salmon begin to experience thermal stress at 18 °C, migration barriers at 20 °C, and mortality at 23 °C (e.g., Keefer et al., 2014; Richter and Kolmes, 2005). Because of this, channel restoration was initiated in 2017 by U.S. Reclamation and completed in December 2019. The restoration goals were to 1) increase hyporheic exchange between the channel and floodplain and 2) provide thermal refuge for migratory and resident Chinook salmon during critical summer months (USBR, 2016). These restoration goals were addressed by constructing a new sinuous channel with

pool-riffle sequences and large wood structures and backfilling the straightened pre-restoration channel. Further, designers constructed a series of morphologic features including alcoves, pools, riffles, bars, and spring channels with the express goals of increasing channel-floodplain hydraulic connectivity and forcing areas of hyporheic and surface water flow convergence in the channel to create thermal refuge for native fish species (USBR, 2016). Spring channels are defined as secondary channels that are disconnected at their upstream end during low-flow conditions and have flow that completely originates from upwelling groundwater. Additionally, alcoves are steep-sided depressions alongside the channel fed partially from groundwater but maintain a surface connection to the main channel. We define thermal refuge as spatially discrete areas that are thermally distinct from the mean water temperature in the river by 0.5° C and below the 18 °C thermal stress threshold for Chinook salmon (e.g., Dugdale et al., 2013; Fakhari et al., 2022; Sullivan et al., 2021). Here we divide specific features by their relative spatial scales, with spring channels, bifurcated channels around an island, and backfilled historic channels considered as valley-scale morphologic features and pools, riffles, alcoves, and bars considered unit-scale features.

2.3 Measurements and techniques

Hourly discharge and water temperatures were monitored at two U.S. Reclamation stream gages located at the top and bottom of the study reach, respectively. Additionally, synoptic discharge surveys were performed throughout the reach during summer low-flow conditions in August of 2021 to evaluate locations of hydrologic gains and losses within the study reach. Discharge surveys were completed using a Sontek Flowtracker2 ADV in a series of cross sections distributed over the length of the study site (Fig. 3).

Groundwater table elevation (GWE) and temperature were continuously monitored since 2018 using an array of 10 observation wells and 3 shallow piezometers (Fig. 1). Wells were drilled along the right floodplain ranging from 4-6 m deep, while the piezometers were manually installed in the left floodplain to a depth of 1 meter. In the wells, water level and temperature were measured every 15 mins with Hobo pressure transducers (+/- 0.05 m and 0.1 °C resolution). The piezometers were fabricated in the laboratory from 1.4 m long PVC pipe. Temperature sensors with 0.006 °C resolution were distributed every 15 cm along the pipe and a pressure transducer with a 0.039 mbar resolution was located at the bottom of the sensor monitored water level. Monthly averaged piezometric head levels and water temperatures in the wells were used to asses groundwater conditions. A cross correlation was performed between the gage height and GWE in each well to determine the lag between changes in stage and GWE. An identical analysis was also performed between the groundwater (GW) and surface water (SW) temperatures.

To evaluate spatial changes in near-bed water temperature in the river and identify potential thermal refuge areas from hyporheic inputs, a longitudinal thermal survey was performed at the same low-flow conditions as the discharge survey. We modified the thermal survey method of Ebersole (2003) to increase the spatial density of measurements in the channel. In each thermal survey, we attached weighted temperature and pressure sensors to the base of a GPS rod via a 15 cm-long cable (see example in Appendix A). The survey was then conducted with three people across the channel simultaneously wading downstream. One person waded along the thalweg and the other two waded along the edges approximately 1 m from the channel banks. Extra time was spent surveying spring channels and alcoves to capture the thermal profile of the entire system. The weighted sensors travelled along the streambed within 15 cm of the RTK GPS sensor and recorded near-bed water temperature and water depth every 10 seconds, which equated to a measurement approximately every 2-2.5 m. Water pressure was corrected for ambient air pressure using a pressure sensor attached to the top of each GPS rod. The temperature accuracy is ± 0.3 °C with a resolution of 0.006 °C and the pressure sensor accuracy is ±0.5 mbar with a resolution of 0.039 mbar. The survey took approximately two hours to complete, so diel warming of approximately 4 °C occurred during the survey. Select temperature probes and tidbits placed throughout the river were used to detrend the diel signal by plotting all water temperatures against the time elapsed during the survey. An exponential function was then fitted to the data ($r^2 = 0.91$) to determine warming per minute for the duration of the survey and then subtracted from the temperature signal in each survey. Temperature and pressure sensors on the GPS rods were calibrated by placing all three sensors in the same location prior to the start and at the end of each survey and shifting the data to account for the 0.45°C and 0.2 mbar offset between temperature and pressure sensors, respectively. Water surface elevation (WSE) was calculated by adding the pressure-calculated depths to the associated RTK GPS elevation during the survey. Due to the dynamic nature of the sensor moving along the streambed and around obstructions in the river, the sensors were occasionally taken out of the water. This led to periodic measurement spikes in pressure and temperature, which were eliminated from the analysis. A Kruskal-Wallis test ($\alpha = 0.05$) was performed to analyze the statistical significance between the median water temperature in each morphologic feature. Additionally, the deepest parts of the pools were sometimes not accessible when the pool depth would submerge the entire GPS unit and were avoided. The pool bottoms were not captured in the thermal surveys but were periodically monitored by fish snorkel surveys performed in late June of 2021 when both discharge and air temperature conditions are similar to our thermal survey, those data are used to supplement our findings (supplementary information). We do not report the fish data, but use their temperature measurements in the deepest sections of the pools that we were not able to measure owing to depths >1 m.

To quantify areas of hydrologic gaining and losing in the river, a valley-scale analysis was performed by comparing GWE in the floodplain and WSE in the channel. A bathymetric LiDAR survey was completed in 2019 and the resulting 1x1 m DEM was used to determine the ground surface elevation at the site. The groundwater table was derived by performing a simple kriging of the GWE in the wells and piezometers. A 2nd order polynomial semivariogram was used to determine the coefficients for the equations solved by the kriging. The WSE in the channel was computed from our thermal survey. Elevations were compared between the GWE and WSE every 2.5 m longitudinally along the length of the channel to determine areas of gaining and losing. Areas where the GWE > WSE were considered gaining sections, while areas where the GWE < WSE were considered losing sections. There is some uncertainty in representing the GWE in the floodplain related to the kriging (standard deviaition = 0.55 m) of the wells and piezometers.

To support the valley-scale gaining and losing analysis and quantify shallow hyporheic fluxes within the channel, 39 hyporheic flux probes were installed in the streambed at various locations throughout the study reach. Due to high flows and vandalism only 11 probes were recovered (Fig. 1). Hyporheic flux probes had similar design, accuracy, and resolution as the piezometers. Two different methods were used to calculate vertical hyporheic flux within the streambed including an analytical method (DeWeese et al., 2017; Luce et al., 2013; 2017) and a local polynomial method with a maximum likelihood estimator from *n* temperature sensors (LPMLEn) (Kampen et al., 2022). The analytical method uses water temperature as a tracer to monitor vertical hydraulic fluxes through the streambed (DeWeese et al., 2017), whereas the LPMLEn estimates vertical flux and thermal diffusivity from streambed temperature using the frequency domain (Kampen et all 2022). The analytical method was used when only 2 temperature sensors are available because LPMLEn method uses at least 3 sensors. These methods were used to compute the vertical hyporheic flux in the streambed every 15 min. Hyporheic flux in each probe was calculated as a point measurement computed over a unit area. Daily, monthly, and seasonal flux averages were analyzed to understand the spatial and temporal variation of hyporheic flux within the streambed.

To address the restoration goal of enhancing hyporheic exchange through constructed morphologic features which induce fluvial hyporheic flow (Tonina and Buffington, 2009; Tonina and Buffington, 2023), we evaluated whether the hyporheic flow induced from the different morphologic features could overwhelm the valley-scale groundwater gradients. First, we compared the direction of flux reported in each probe to the direction of flux expected from the valley-scale groundwater gradients. If these did not match, we then compared the direction of flux reported in the probe to the direction of flux expected from the morphologic feature surrounding the probe. We used the findings of Gariglio

et al. (2013) to define the expected direction of each geomorphic feature. If the direction of flux in the probe did not match the result of the valley-scale groundwater analysis but was in accord with what was expected from the morphologic feature, it was considered a case where the flux induced from the morphologic feature overwhelmed the hyporheic flux from the groundwater conditions.

3. Results

3.1 Valley-scale features driving hyporheic and thermal conditions

Surface-water temperatures vary seasonally, with winter water temperatures near 0 °C and summer temperatures reaching 26 °C (Fig. 2a). Surface-water temperatures during late summer are well above the 18 °C stress threshold for Chinook salmon from approximately June to late August, and above the mortality threshold (23 °C) for July and early August. Groundwater temperatures are coldest in March (~7 °C) and warmest in September (~15 °C). Cross correlation results show that there is a temporal lag between surface-water temperature and groundwater temperature of 36 days. Consequently, the groundwater is cooler than the surface water from late may to September, whereas the opposite is true from October to March (Fig. 2a). Therefore, groundwater only has the potential to cool the surface water from late may to September, which defines the period that groundwater-driven thermal refuge is possible in the system. The creation of cool thermal refuge in the channel is only possible if the groundwater temperature is cooler than the surface water and the groundwater fluxes are of sufficient magnitude. During the low-flow survey, river stage at the upstream gage was 0.04 m, whereas during peak flows in April the river stage was 0.90 m, an annual stage fluctuation of 0.86 m which is ~78% of bankfull depth . Average annual groundwater levels fluctuate by 0.99 m throughout the year, with minimum groundwater levels occurring in August and maximum water levels occurring in April similar to the SW conditions. The cross correlation of river stage and GWE suggest that seasonal changes in stage are quickly reflected (~1 day) in groundwater levels, while the cross correlation of SW temperature and GW temperature report a lag of 36 days. When river stage increases the SW in the channel displaces water in the adjacent floodplain and immediately increases the fluid pressure in the floodplain, resulting in the 1-day lag between river stage and GWE. While the 38-day lag between GW and SW temperatures exists because it takes 38 days for the surface water to reach the wells in the floodplain. This rapid response between GW and SW levels indicates changes in head propagate rapidly through the floodplain. However, during summer low flows, the SW and GW level fluctuations are small. In August, average SW level variations at the gage are 0.05 m and 0.15 m in the wells, indicating the SW and GW conditions are very stable during the low-flow period. Because of the stability during low flow, we believe our results from our thermal survey in august are representative of the hydraulic conditions of the reach during all low-flow conditions.

To examine the cumulative effects of gaining and losing conditions through the reach, we compared flow at the upstream and downstream gages. On the date of our survey, flow measured at the upstream and downstream gages was 0.335 m^3/s and 0.326 m^3/s, respectively, which was less than a 3% difference and within the error of the instruments. This indicates that the reach as a whole is neither gaining nor losing. This is consistent over the entire low-flow period from early-July to mid-October, when the percent difference between gages remains less than 8%. However, the spatial discharge survey indicates that locally, SW is both gained and lost from the channel over the extent of the reach. Results from the valley-scale groundwater analysis demonstrate that the valley-scale hyporheic exchange has substantial spatial variability throughout the reach (Fig. 3). During low-flow conditions, the vertical head difference between the GW and SW spatially range from -1 m to 1.3 m throughout the reach, where locations with the largest head differentials identify the strongest GW-SW exchange. Both spring channels (Figure 1 inserts red and blue; Figure 3) are disconnected from the main channel at the upstream end, so all water within the channels is derived from upwelling hyporheic flow.

During the stable low flows, the discharge survey indicates that a substantial amount of the SW is lost or gained throughout the reach in the form of hyporheic exchange, with different morphologic features affecting the flow losses and gains (Fig. 3). Results from both the valley-scale GW analysis and discharge surveys suggest that the backfilled historic channel induces the most substantial GW-SW exchange in the reach during low flows. Measured losses during the discharge survey suggests SW in the main channel enters the inactive backfilled channel in the form of hyporheic flow (Fig. 3). Just upstream of the backfilled channel, discharge was measured at 0.46 m^3/s, whereas immediately downstream of the entrance to the backfilled channel the discharge drops to 0.33 m^3/s, a flow reduction of 0.13 m^3/s. Farther downstream, measured discharge before (0.32 m^3/s) and after (0.47 m^3/s) the backfilled channel meets the main channel, indicates a flow increase of 0.15 m^3/s. The volumetric losses through the backfilled channel constitute approximately 30% of the surface water in the main channel immediately upstream of the old channel and 43% of the flow at the upstream gage. This reduction in discharge observed in the main channel near the upstream boundary of the backfilled channel is in agreement with the GW-SW comparison, which show that groundwater levels near that location are more than 0.8 m below the surface-water elevations (Fig. 3). The strongest gaining conditions in the reach were measured at the downstream boundary of the backfilled channel and correspond to the valley-scale groundwater analysis that shows groundwater elevations that are more than 1 m above the surface-water elevations. These results suggest that a substantial percentage of the total SW flow in the channel can be passed through valley-scale subsurface geomorphic features like the backfilled channel before returning to the main channel.

3.2 Unit-scale features driving hyporheic and thermal conditions

The hyporheic flux probes illustrate temporal variation in the hyporheic fluxes through specific morphologic features over the course of a year (Appendix A). Hyporheic fluxes in the streambed have an annual range from 3.01×10^{-5} to -2.8×10^{-5} m/s and depend on the season. The highest magnitude fluxes occur during the months of April and May, which correspond to peak SW flows. Comparing the point measurements of the hyporheic flux probes to the valley-scale groundwater analysis during low flows shows that 10 probes agree with the broader valley-scale GW-SW gradients, indicating that GW-SW may overwhelm fluvial hyporheic exchange due to local features (Table 1). The directions of hyporheic fluxes estimated in the probes match the direction of fluxes expected from the groundwater gradients for all probes, apart from probe 22. Probe 22 reports moderate upwelling flux of 4.45×10^{-6} m/s, while the valley-scale groundwater analysis indicates downwelling. Because probe 22 is located in a plane bed morphology, the bed morphology is not expected to drive substantial hyporheic flow. In this case, we attribute the disagreement between the probe results and valley-scale groundwater results to the orientation of the probe, which was unintentionally installed at an angle and leads to uncertainty in the flux estimation. All other probes reported flux directions that agree with the valley-scale groundwater results. Probe 3 is located in a pool head where hyporheic upwelling is expected. However, flux values in the probe show downwelling fluxes of -3.04×10^{-6} m/s which match the direction of the GW-SW analysis. Downwelling at this location is in accord with the valley-scale groundwater analysis, this indicates groundwater gradient is stronger than gradients due to flow-bedform interaction. In comparison, probe 7, also located in a pool head, has both GW-SW gradients and the probe showing upwelling. In cases where the hyporheic flow direction agrees with both the expected morphologic effect and the valley-scale groundwater gradient, we are unable to separate and quantify the individual contributions of the morphologic unit and groundwater gradient.

The median flux magnitude of all probes is 6.49×10^{-6} m/s during the entire year. However, during low flow the median measured hyporheic fluxes in each probe decrease to 3.46×10^{-6} m/s. The mean area of the unit-scale features (pools, bars, riffles, and alcoves) within the study reach is 325 m^2. Using the median flux from the probes during low flow and the average feature size, the hyporheic flow contribution of a single average morphologic feature in the study reach is estimated to be less than 8.84×10^{-4} m^3/s, which accounts for less than 0.4 % of total stream discharge during low-flow conditions If the maximum flux values during low flow are used in this calculation, the hyporheic flow contribution is still less than 2% of total stream flow. Fluxes of this magnitude do not appear to be capable of generating localized thermal refuge, as shown by the observed water temperatures around upwelling probes. Of the nine probes reporting hyporheic upwelling from the streambed, only

probe 23, which is located in a pool tail, observes a change in temperature > 0.5 °C that is considered thermal refuge. In probe 23, near-bed water temperatures stay below 14.9 °C within an area of 30 m^2 surrounding the probe. During low-flow conditions, the median flux magnitude in probe 23 is 1.03 x 10^{-6} m^3/s per unit area, which is well below the median low flow flux of all the other probes. The valley-scale groundwater analysis also reports minimal gaining at this location with a GW-SW head gradient of less than 0.2 m. This suggests that fluxes of this magnitude alone are not substantial enough to generate localized thermal refuge with the available thermal gradient between the GW and SW.

3.3 Geomorphic features maintaining thermal refuge

The longitudinal thermal survey illustrates that individual morphologic features maintain distinct temperature ranges (Fig. 4). Spring channels had a median temperature of 15.8 °C ($p > 0.05$) and the greatest temperature variability of all features with an inner quartile range of 1.7 °C (Fig. 4). Because all flow in these channels originates from hyporheic flow the upper boundary is low temperature. However, flows in these channels are relatively slow moving (~0.005 m/s) and shallow (~5-20 cm). Therefore, rapid warming occurs in the downstream direction. Water temperatures in one spring channel increase linearly with distance downstream, beginning at 13.9 °C at the upstream boundary of the channel and increasing to 18.3 °C at the downstream end near the confluence with the main channel (Fig. 5a). In another spring channel, we were only able to measure its downstream section because of large wood in the channel, but water temperatures also increased approximately linearly from 15.6 °C to 17.6 °C (Fig. 5b). This is an increase of 4.4 °C over 112 m in the first channel and 2 °C over 36 m in the second channel. In both channels, water temperature increases to near or above the stressful temperature threshold (18 °C) before it enters the main channel. The spring channel in figure 5b intersects and follows the path of the historic backfilled channel before exiting into the main channel, resulting in an influx of warm surface water into the main channel. Water temperatures in the pool at the downstream convergence of the backfilled channel and main channel are highly variable, ranging from 13.7 °C in the right margin of the pool to 18.1 °C along the left margin of the pool(Fig. 6). Cool temperatures here are likely driven from subsurface flows through the backfilled channel, while warm temperatures here are likely driven by the surface water from the spring channel.

The median water temperature from all thermal survey measurements in the reach was 15.4 °C. In comparison, pools have the lowest median temperature of 14.9 °C ($p < 0.001$) and are the only feature with a median temperature that satisfies the thermal refuge condition. Additionally, pools show the least variability of all the features with an inner quartile range of 0.3 °C. The comparison of the pool bottom elevations to the adjacent GWE in the floodplain indicates that the bottom elevation of each

pool was greater than 1 m below the GWE, suggesting that the pools are hydraulically connected to the water table in the study reach. The groundwater table slopes downward in the southeast direction across the reach and the orientation of the slope is nearly perpendicular to more than half of the pools. This suggests that ambient groundwater underflow driven by valley slow does intersect those pools, and potentially helps maintain cool temperatures in the pools. Riffles also have low temperature variability with an inner quartile range of 0.6 °C and the second lowest median water temperature of 15.3° C ($p < 0.05$), but the temperature differential was limited and did not meet the thermal refuge criterion (Fig. 4). The low water temperatures in the riffles likely occur because many riffles are located downstream of pools and receive a portion of the cool water exiting the pool. In comparison, alcoves showed greater variability in temperature than pools and riffles (inner quartile range of 0.8 °C) and were one of the warmest features with a median temperature of 15.7° C ($p<0.05$). While these features are adjacent to the channel, they have near-stagnant velocities during low flows and may not exchange water freely with the main channel. Therefore, they are warmer than the main channel because of low mass exchange and shallow depths. Plane bed and bar morphologies show little difference from the median channel temperature with inner quartile ranges of less than 0.6 °C and median temperatures of 15.7 °C ($p>0.05$) and 15.5 °C ($p<0.05$), respectively.

4. Discussion

4.1 Valley-scale hyporheic and thermal conditions

At the GRR study site, thermal refuge for fish is most important from mid-June through August when temperatures rise above thermal stress thresholds (Fig 2a). Conditions for potential thermal refuge exist from early June to September when the groundwater is cooler than the surface water, so hyporheic flow could provide a cooling mechanism. However, there must be hydraulic connectivity between the surface and groundwater so that hyporheic exchange can occur and generate thermal refuge. Our results show strong hydraulic connectivity between the river and floodplain as changes in river stage are quickly reproduced in the groundwater levels (Fig. 2b). The rapid response in the water table occurs in the coupled river-floodplain system of the GRR corridor because the subsurface alluvial floodplain material is a mixture of gravel and sand, which typically have relatively high hydraulic conductivity values compared to finer floodplain sediments (Freeze and Cherry, 1979; Harter, 2003; Heath, 1983). Floodplain connectivity and hyporheic flux rates are partially dependent on hydraulic conductivity. Similar rapid responses in floodplain groundwater levels have been observed in other semi-confined mountain river systems with high stream power where valley material has high conductivity (e.g., Kasahara and Wondzell, 2003; Poole et al., 2006; Benjankar et al., 2020). In contrast, floodplains like those in many lowland rivers may experience limited

fluctuations in groundwater levels when compared to river stage (Marchand et al., 2022). While semi-confined mountainous streams with high stream power have high sediment transport capacity and competence that can mobilize large grain sizes, unconfined lowland rivers with low stream power transport much finer grain sizes (Ali et al., 2013; Bizzi and Lerner, 2015) and deposit a higher percentage of fines through the river corridor (Beuselinck et al., 2002) that results in lower hydraulic conductivity values and associated hyporheic exchange rates (Malenda et al., 2019; Nowinski et al., 2011). Restoration designs that intend to enhance floodplain connectivity and hyporheic fluxes should clearly define how restoration goals fit into the existing floodplain framework; factors such as recharge inputs and floodplain material and associated hydraulic conductivity should all be considered.

4.2 Performance of valley-scale and unit-scale morphologic units to induce hyporheic flow

Results from this study imply that the backfilled channel is a principal driver of hyporheic exchange within the study site. Our results indicate that up to 30% of the surface water at low flows from the main channel is expected to flow into the subsurface in the form of hyporheic flow and emerges from the lower portion of the historic backfilled channel. These findings imply that the backfilled channel is a principal driver of hyporheic exchange in the floodplain and accommodates substantial quantities of surface water exchange, likely due to higher hydraulic conductivity from unconsolidated sediment (e.g., Hester et al., 2020; Samadder et al., 2011; Schilling et al., 2022). This is consistent with previous studies that show surface water from the main channel can penetrate the aquifer and follow subsurface hyporheic flow paths into adjacent side channels (e.g., Kasahara and Wondzell, 2003; Jones et al., 2008). Jones et al., 2008, showed that up to 20% of the water found in an adjacent spring channel was originally derived from the main channel. Additionally, other studies have shown that complex hydrologic mechanisms beneath abandoned side channels continue to operate irrespective of backfilling (Marchand et al, 2002). However, it is uncertain if this elevated hydraulic conductivity will change over time as settling, interstitial pore clogging, and organic material infiltration via roots and decomposition will affect these subsurface flow paths (e.g., Brantley et al., 2017; Newman et al., 2004). Regardless, our results suggest that hyporheic exchange through abandoned or backfilled channels can account for ~30% of SW flow in some situations. Additionally, hyporheic flows exiting the downstream end of the backfilled channel are 13% greater than those entering it at the upstream end, potentially indicating that these large-scale features with high hydraulic conductivities relative to the surrounding sediment can act as subsurface drains and concentrate flow paths at their discharge point. However, the surface flow in the spring channel intercepts and follows the path of the backfilled channel, resulting in the downstream mixing of cool water flowing beneath the backfilled channel and warm surface water from the spring channel(Fig. 6). This complex mixture of surface

and subsurface flows may limit the thermal refuge potential from cool subsurface flows at the exit of the backfilled channel. Other studies have shown that complex mixing patterns at the confluence of main channels and secondary channels can result in highly variable water temperatures (e.g., Lambs, 2004; Lewis and Rhoads, 2015; Yuan et al., 2022). The wide range of temperatures and lack of thermal refuge here can be attributed to these complex mixing patterns. Therefore, river restoration designs intended to incorporate constructed or paleochannel features to enhance large-scale hyporheic exchange should attempt to connect flow paths in abandoned channels and/or adjacent backfilled channels while avoiding convergence with warm surface water (e.g., Jones et al., 2008; Tranmer et al., 2022).

In the GRR, the restoration design expectation was that each unit-scale morphologic feature would enhance hyporheic flow and generate local thermal benefits (USBR, 2016). For example, upwelling was expected in the pool heads, while the pool tails were expected to induce downwelling conditions (e.g., Crispell and Endreny, 2009; Gariglio et al., 2013). However, it was unknown whether the hyporheic fluxes generated from these unit-scale features could overwhelm the valley-scale groundwater gradients. We found that regardless of the monitored unit-scale morphologic feature, none of the unit-scale features could generate hyporheic fluxes counter to the valley-scale groundwater gradients. This is consistent with other studies that show gaining and losing fluxes from the valley-scale groundwater may dominate and remove fluvial hyporheic exchange (Fox et al., 2014; Malzone et al., 2016; Sawyer and Cardenas, 2012), because for a unit-scale feature to dominate hyporheic processes, the valley-scale GW-SW head gradients must be below a minimum threshold value (e.g., Marzadri et al., 2016). Previous studies indicate that under gaining conditions groundwater upwelling reduces the penetration of SW into the streambed, diminishing the strength of bedform-driven hyporheic fluxes and reducing the vertical extent of the hyporheic zone beneath the streambed (Boano et al., 2008; Hester and Doyle, 2008). In contrast, during losing conditions the hyporheic exchange with the streambed is reduced by the redirecting a portion of the surface water in the hyporheic zone farther into the deeper groundwater when it would have previously returned to the stream (Fox et al., 2014). Since hyporheic exchange with the streambed is reduced by different processes under losing and gaining conditions, the minimum GW-SW head gradient might be different for each condition. Regardless, we found that under both gaining and losing conditions, none of the unit-scale morphologic features monitored by the hyporheic flux probes were able to overwhelm the valley-scale groundwater gradients. This inability of unit-scale features to overwhelm valley-scale GW-SW gradients limits the design efficacy of restoration practitioners attempting to use unit-scale features to enhance hyporheic exchange. Therefore, an understanding of the valley-scale

flow field is critical to understand prior to restoration design so that it can help guide the placement of specific morphologic features.

4.3 Identification of Thermal Refuge

Results from the thermal survey suggest that pools and riffles had the lowest water temperatures of all the constructed morphologic features, but only pools achieved the >0.5 °C difference from the median stream temperature. Because our wading survey did not measure the deepest portions of pools that were > 1 m deep, it is likely that water temperatures at the bottom of the pools were colder than we reported. Thus, we consider our results to be an indicator of thermal habitat. In fact, during fish snorkel surveys in the reach some pools maintained water temperatures that were ~3 °C cooler than the surrounding channel temperature (see Appendix A). From the perspective of thermal refuge and habitat, deep pools have been found to both maintain cooler temperatures and provide thermal refuge (e.g., Torgerson et al., 1999). Our results found pools are typically the only unit-scale feature able to reliably provide thermal refuge. Here, they did not overwhelm valley-scale groundwater gradients, but incorporate them for thermal benefit. The mechanisms suggested to maintain pool temperatures cooler than other parts of the channel include increased thermal protection from solar radiation, the retention of lateral and/or vertical groundwater seepage in the low velocity portion of the pool, and the accumulation of vertical hyporheic flow induced by a geomorphic feature at the bottom of the pool (e.g., Hassan et al., 2015; Tate et al., 2005). These mechanisms are supported by our finding that the bottom elevations of all the pools were below the GWE in the adjacent floodplain, indicating that the pool bottoms penetrate the aquifer. We are not able to determine which mechanism is the primary driver in each pool, but we hypothesize some combination of these mechanisms leads to reduced temperatures in the pools. We acknowledge that if water temperatures reach 23 °C as they do in this reach, the thermal refuge criterion of 0.5 °C will not maintain suitable temperatures for Chinook salmon. However, this may be valuable to extend the spring and fall rearing periods when a temperature difference of 0.5 °C in these reaches as well as allow migratory fish to have resting areas during critical migration periods.

Our thermal survey results suggest that spring channels at the study site had potential for generating thermal refuge, but longitudinal warming causes a thermal barrier in the channels during critical times of the year that limits access to the thermally suitable portion in the upstream sections of the channels. In the GRR, the shallow, low-velocity spring channels showed the greatest temperature variability of all features. This variability occurs because cool water derived from valley-scale gradients at the upstream boundary of the spring channels warms in the downstream direction. The spring channels at our site are shallow, poorly shaded, and low velocity, making them susceptible to warming. A

modeling study demonstrated that an 80% shade reduction in low-velocity (0.023 m/s) channels can result in a 5.4 °C increase in mean stream temperatures in a 1 km reach (Garner et al., 2017). The same 80% shade reduction was analyzed at high velocity (0.155 m/s), and mean water temperatures only increased by 1.6 °C. This indicates that channel velocity plays a critical role in preserving cooler temperatures in unshaded channels. This is problematic for most spring-fed channels because they are generally low velocity features derived from hyporheic flow. Additionally, studies have determined that small streams with shallow depths (~0.15 m) are also susceptible to warming from solar radiation when riparian shading is limited (e.g., Johnson and Jones, 2000; Rutherford et al., 2004; Moore et al., 2005; Studinski et al., 2012). In our spring channels, water temperatures increased by 3.7-5.1 °C per 100 m, which is higher than most previous studies. For example, Rutherford et al. (2004) found a shallow (~0.15 m) stream warmed at a rate of 0.66 °C/100 m when riparian shade was reduced by 40% and Studinski et al. (2012) observed 0.18-0.79 °C / 100 m with 50-90% riparian thinning. Our results in the GRR indicate that spring channels have the potential to generate substantial thermal refuge, but warming mechanisms of shallow depths, low velocities, and lack of riparian shading are compounded to make them highly susceptible to warming. Collectively, these findings indicate that riparian shade is a critical component to maintain acceptable local water temperatures and thermal refuge in shallow, slow-moving secondary channels. To increase thermal refuge potential in secondary and spring channels, restoration designs could implement narrower, deeper secondary channels and ensure sufficient riparian vegetation cover to help maintain cooler water temperatures. While there are significant riparian plantings along the streambanks and floodplain in the GRR restoration reach (USBR, 2018), there is a temporal lag between plant establishment, growth, and shading benefits to the channel (e.g., Bendix and Cowell, 2010; Bess et al., 2002; Tranmer et al., 2020). Therefore, secondary channels should not expect to provide hydraulically connected thermal refuge areas until the riparian canopy can develop, which may occur 3-15 years after restoration construction is completed depending on plant species (Galatowitsch and Richardson, 2005; Lennox et al., 2011; Gardiner et al., 2004; Sigurdsson et al., 1998)

Hyporheic upwelling from the streambed has the potential to generate thermal refuge (Boano et al., 2008) but the conditions under which that is possible are still uncertain (Arrigoni et al., 2008; Schmadel et al., 2016). To understand the spatial extent of thermal refuge from upwelling, we inspected water temperatures near all the hyporheic flux probes that reported upwelling. Unfortunately, results from our thermal survey indicate that only near-bed temperatures around probe 23, which resides in a pool, were cool enough to be considered thermal refuge. The magnitude of hyporheic fluxes coming from the streambed near probe 23 are marginal compared to the streamflow (<0.001%), making it unlikely that hyporheic flow alone is driving cooler temperatures at this

location. Cool temperatures around this probe can be attributed to the mechanisms we suggest that regulate pool temperature, which include protection from solar radiation, the retention of lateral and/or vertical groundwater seepage into the bottom of the pool, and the accumulation of vertical unit-scale hyporheic flow induced at the bottom of the pool. Broadening our results to the entire reach demonstrates that average hyporheic flow induced by a single feature constitutes less than 0.03% of the total discharge in the channel during summer low-flow conditions, which appears to be insufficient to provide localized thermal refuge within the channel. Similar findings were observed in previous studies when no thermal refuge formed at locations where the total hyporheic flow contribution from a feature was less than 2% of the total streamflow (Sawyer and Cardenas, 2012; Sawyer et al., 2012). Therefore, the availability of thermal refuge within a given system is likely a function of the magnitude of hyporheic upwelling and relative temperature difference between the surface and groundwater (e.g., Hester and Gooseff, 2011, sawyer et al., 2012; Arrigoni et al., 2008). Additionally, cooling from each hyporheic input is cumulative within the reach and restoring channels with a greater number of features that enhance hyporheic exchange could still benefit instream temperatures (e.g., Menichino and Hester, 2014; Arrigoni et al., 2008). However, bulk cooling of the channel is still limited as water temperatures in the main channel were reduced by less than 0.25 °C after restoration in both Sawyer and Cardenas (2012) and Sawyer et al. (2012). Our results suggest that from a mass exchange perspective, the larger valley-scale features such as backfilled channels and spring channels may be more effective than a number of small features. However, even with these larger features that facilitate high surface-groundwater exchange, bulk cooling of the water in the main channel could be limited. Therefore, more studies are needed to determine what percentage of the total streamflow must be generated by hyporheic flow to create areas of thermal refuge.

In this study, we propose a simple thermal monitoring approach in wadable rivers to capture high-resolution, instream temperature data for the identification of thermal refuge. This method combines two readily available technologies, RTK GPS and continuously recording pressure and temperature sensors to map near-bed water temperatures through a 2.5 km long reach with complex morphology in less than two hours. Here we attached custom-built thermistors and transducers from our laboratory to a GPS unit, but this method could also use any combination of commercial temperature sensor and pressure transducer capable of monitoring water temperature and depth at 5-10 sec intervals. Those measurements can then be directly linked to GPS locations using the timestamp. This approach builds on the method of Ebersole (2003) who manually collected temperature data at set 5 m intervals in the channel. Our method provides a means to rapidly measure wadable streams with greater mobility to monitor areas within the channel. For example, the thermal survey capturing the 30 m^2 of cool water

surrounding probe 23 allowed for the spatial extent of the thermal refuge to be identified and mapped. Some error is introduced into these measurements when the sensor is taken out of the water to avoid instream obstacles, but those data can be easily identified by the pressure signature. Once the data points where the sensor was taken off the bed were removed, the RMSE between the survey elevation and the DEM was 0.12 m. Even when the GPS rod is not exactly on the streambed, the weighted sensor remains on the bed owing to the flexible cable.

5. Conclusion

The overall effectiveness of river restoration by increasing hyporheic flows on forming thermal refuge has been called into question over claims that large-scale environmental drivers such as flow regime, existing groundwater conditions, and surrounding lithology often overshadow the potential effects of locally placed in-stream structures. To address this, we evaluate a suite of constructed morphologic features in a recently restored river reach to determine their efficacy in generating hyporheic flows and creating thermal refuge during critical summer low-flow months. We do this using our newly proposed thermal monitoring approach in wadable rivers that captures high-resolution, instream temperature data for the identification of thermal refuge. The study reach exhibits strong hydraulic connectivity with the floodplain as river stage changes propagate rapidly through the floodplain, changing the groundwater table levels by a similar magnitude. Our results show hyporheic flow from most morphologic features have insufficient magnitudes relative to the total streamflow to provide thermal refuge. Additionally, we see in most cases that valley-scale groundwater gradients do not allow the formation of fluvial hyporheic flows induced by a unit-scale features, e.g., pool-riffle.

Pools were the only unit-scale morphologic feature that provided significant thermal refuge of 0.5° C. This is due to the suggested mechanisms of thermal buffering from solar radiation and the accumulation of cool hyporheic flow in the low velocity portion of the pool. Spring channels provide cool water temperatures, but warm downstream due to shallow depths, low velocities, and lack of shade. This effectively creates a thermal barrier near the downstream end of these channels that precludes their use as thermal refuge. Understanding which constructed morphologic features are effective at creating thermal refuge is critically important for habitat-based restoration. Our findings on the generation and preservation of thermal refuge can be used to inform the design of future river restoration projects. Future research should investigate 1) what percentage of the total streamflow must hyporheic flow contribute to create and sustain localized thermal refuge, and 2) what pool characteristics (e.g, maximum depth, pool volume, surface area, etc.) are most important for creating and maintaining thermal refuge.

References

Ali, M., Seeger, M., Sterk, G., & Moore, D. (2013). A unit stream power based sediment transport function for overland flow. *CATENA*, *101*, 197-204.

Arrigoni, A. S., Poole, G. C., Mertes, L. A. K., O'Daniel, S. J., Woessner, W. W., & Thomas, S. A. (2008). Buffered, lagged, or cooled? Disentangling hyporheic influences on temperature cycles in stream channels. *Water Resources Research*, *44*(9).

Bakke, P. D., Hrachovec, M., & Lynch, K. D. (2020). Hyporheic process restoration: design and performance of an engineered streambed. *Water*, *12*(2), 425.

Beechie, T., Imaki, H., Greene, J., Wade, A., Wu, H., Pess, G., Roni, P., Kimball, J., Stanford, J., Kiffney, P., & Mantua, N. (2013). RESTORING SALMON HABITAT FOR A CHANGING CLIMATE. *River Research and Applications*, *29*(8), 939-960. https://doi.org/https://doi.org/10.1002/rra.2590

Beechie, T. J., Sear, D. A., Olden, J. D., Pess, G. R., Buffington, J. M., Moir, H., Roni, P., & Pollock, M. M. (2010). Process-based principles for restoring river ecosystems. *BioScience*, *60*(3), 209-222.

Bendix, J., & Cowell, C. M. (2010). Impacts of Wildfire on the Composition and Structure of Riparian Forests in Southern California. *Ecosystems*, *13*(1), 99-107.

Benjamin, J. R., Bellmore, J. R., Whitney, E., & Dunham, J. B. (2020). Can nutrient additions facilitate recovery of Pacific salmon? *Canadian Journal of Fisheries and Aquatic Sciences*, *77*(10), 1601-1611.

Bess, E. C., Parmenter, R. R., Mccoy, S., & Molles, M. C. (2002). Responses of a Riparian Forest-Floor Arthropod Community to Wildfire in the Middle Rio Grande Valley, New Mexico. *Environmental Entomology*, *31*(5), 774-784.

Beuselinck, L., Hairsine, P. B., Govers, G., & Poesen, J. (2002). Evaluating a single-class net deposition equation in overland flow conditions. *Water Resources Research*, *38*(7), 15-11-15-10.

Bizzi, S., & Lerner, D. N. (2015). The Use of Stream Power as an Indicator of Channel Sensitivity to Erosion and Deposition Processes. *River Research and Applications*, *31*(1), 16-27.

Boano, F., Revelli, R., & Ridolfi, L. (2008). Reduction of the hyporheic zone volume due to the stream-aquifer interaction. *Geophysical Research Letters*, *35*(9).

Brantley, S. L., Eissenstat, D. M., Marshall, J. A., Godsey, S. E., Balogh-Brunstad, Z., Karwan, D. L., Papuga, S. A., Roering, J., Dawson, T. E., Evaristo, J., Chadwick, O., McDonnell, J. J., & Weathers, K. C. (2017). Reviews and syntheses: on the roles trees play in building and

plumbing the critical zone. *Biogeosciences*, *14*(22), 5115-5142. https://doi.org/10.5194/bg-14-5115-2017

Crispell, J. K., & Endreny, T. A. (2009). Hyporheic exchange flow around constructed in-channel structures and implications for restoration design. *Hydrological Processes*, *23*(8), 1158-1168.

DeWeese, T., Tonina, D., & Luce, C. (2017). Monitoring streambed scour/deposition under nonideal temperature signal and flood conditions. *Water Resources Research*, *53*(12), 10257-10273.

Dugdale, S. J. (2016). A practitioner's guide to thermal infrared remote sensing of rivers and streams: recent advances, precautions and considerations. *WIREs Water*, *3*(2), 251-268.

Dugdale, S. J., Bergeron, N. E., & St-Hilaire, A. (2013). Temporal variability of thermal refuges and water temperature patterns in an Atlantic salmon river. *Remote Sensing of Environment*, *136*, 358-373.

Eaton, J. G., & Scheller, R. M. (1996). Effects of climate warming on fish thermal habitat in streams of the United States. *Limnology and Oceanography*, *41*(5), 1109-1115.

Ebersole, J. L., Liss, W. J., & Frissell, C. A. (2003). COLD WATER PATCHES IN WARM STREAMS: PHYSICOCHEMICAL CHARACTERISTICS AND THE INFLUENCE OF SHADING1. *JAWRA Journal of the American Water Resources Association*, *39*(2), 355-368.

Fakhari, M., Raymond, J., Martel, R., Dugdale, S. J., & Bergeron, N. (2022). Identification of Thermal Refuges and Water Temperature Patterns in Salmonid-Bearing Subarctic Rivers of Northern Quebec. *Geographies*, *2*(3), 528-548.

Favrot, S. D., Jonasson, B. C., & Peterson, J. T. (2018). Fall and Winter Microhabitat Use and Suitability for Spring Chinook Salmon Parr in a U.S. Pacific Northwest River. *Transactions of the American Fisheries Society*, *147*(1), 151-170.

Fox, A., Boano, F., & Arnon, S. (2014). Impact of losing and gaining streamflow conditions on hyporheic exchange fluxes induced by dune-shaped bed forms. *Water Resources Research*, *50*(3), 1895-1907.

Galatowitsch, S., & Richardson, D. M. (2005). Riparian scrub recovery after clearing of invasive alien trees in headwater streams of the Western Cape, South Africa. *Biological Conservation*, *122*(4), 509-521.

Gardiner, E. S., Stanturf, J. A., & Schweitzer, C. J. (2004). An Afforestation System for Restoring Bottomland Hardwood Forests: Biomass Accumulation of Nuttall Oak Seedlings Interplanted Beneath Eastern Cottonwood. *Restoration Ecology*, *12*(4), 525-532.

Gariglio, F. P., Tonina, D., & Luce, C. H. (2013). Spatiotemporal variability of hyporheic exchange through a pool-riffle-pool sequence. *Water Resources Research*, *49*(11), 7185-7204.

Garner, G., Malcolm, I. A., Sadler, J. P., & Hannah, D. M. (2017). The role of riparian vegetation density, channel orientation and water velocity in determining river temperature dynamics. *Journal of Hydrology*, *553*, 471-485.

Goniea, T. M., Keefer, M. L., Bjornn, T. C., Peery, C. A., Bennett, D. H., & Stuehrenberg, L. C. (2006). Behavioral thermoregulation and slowed migration by adult fall Chinook salmon in response to high Columbia River water temperatures. *Transactions of the American Fisheries Society*, *135*(2), 408-419.

Greer, G., Carlson, S., & Thompson, S. (2019). Evaluating definitions of salmonid thermal refugia using in situ measurements in the Eel River, Northern California. *Ecohydrology*, *12*(5), e2101.

Harter, T. (2003). *Basic concepts of groundwater hydrology*. UCANR Publications.

Hassan, M. A., Tonina, D., Beckie, R. D., & Kinnear, M. (2015). The effects of discharge and slope on hyporheic flow in step-pool morphologies. *Hydrological Processes*, *29*(3), 419-433.

Heath, R. (1983). Basic ground-water hydrology, USGS Water Supply Paper 2220. *US Geol. Surv., Reston, Va*.

Hester, E. T., & Doyle, M. W. (2008). In-stream geomorphic structures as drivers of hyporheic exchange. *Water Resources Research*, *44*(3).

Hester, E. T., & Fox, G. A. (2020). Preferential Flow in Riparian Groundwater: Gateways for Watershed Solute Transport and Implications for Water Quality Management. *Water Resources Research*, *56*(12), e2020WR028186.

Hester, E. T., & Gooseff, M. N. (2011). Hyporheic restoration in streams and rivers. *Stream restoration in dynamic fluvial systems: Scientific approaches, analyses, and tools*, *194*, 167-187.

Isaak, D. J., Luce, C. H., Horan, D. L., Chandler, G. L., Wollrab, S. P., & Nagel, D. E. (2018). Global Warming of Salmon and Trout Rivers in the Northwestern U.S.: Road to Ruin or Path Through Purgatory? *Transactions of the American Fisheries Society*, *147*(3), 566-587.

Isaak, D. J., Young, M. K., Luce, C. H., Hostetler, S. W., Wenger, S. J., Peterson, E. E., Ver Hoef, J. M., Groce, M. C., Horan, D. L., & Nagel, D. E. (2016). Slow climate velocities of mountain streams portend their role as refugia for cold-water biodiversity. *Proceedings of the National Academy of Sciences*, *113*(16), 4374-4379.

Jones, K. L., Poole, G. C., Woessner, W. W., Vitale, M. V., Boer, B. R., O'Daniel, S. J., Thomas, S. A., & Geffen, B. A. (2008). Geomorphology, hydrology, and aquatic vegetation drive seasonal hyporheic flow patterns across a gravel-dominated floodplain. *Hydrological Processes*, *22*(13), 2105-2113.

Kasahara, T., & Wondzell, S. M. (2003). Geomorphic controls on hyporheic exchange flow in mountain streams. *Water Resources Research*, *39*(1), SBH 3-1-SBH 3-14.

Keefer, M. L., Clabough, T. S., Jepson, M. A., Johnson, E. L., Peery, C. A., & Caudill, C. C. (2018). Thermal exposure of adult Chinook salmon and steelhead: Diverse behavioral strategies in a large and warming river system. *PLOS ONE*, *13*(9), e0204274.

Keefer, M. L., Clabough, T. S., Jepson, M. A., Naughton, G. P., Blubaugh, T. J., Joosten, D. C., & Caudill, C. C. (2015). Thermal exposure of adult Chinook salmon in the Willamette River basin. *Journal of Thermal Biology*, *48*, 11-20.

Kurylyk, B. L., MacQuarrie, K. T. B., Linnansaari, T., Cunjak, R. A., & Curry, R. A. (2015). Preserving, augmenting, and creating cold-water thermal refugia in rivers: concepts derived from research on the Miramichi River, New Brunswick (Canada). *Ecohydrology*, *8*(6), 1095-1108.

Lambs, L. (2004). Interactions between groundwater and surface water at river banks and the confluence of rivers. *Journal of Hydrology*, *288*(3), 312-326.

Legg, N., Ybarrondo, M. (2015). *Draft Hydrologic Analysis for the Bird Track Restoration Project*. Cardno Design Services

Lennox, M. S., Lewis, D. J., Jackson, R. D., Harper, J., Larson, S., & Tate, K. W. (2011). Development of Vegetation and Aquatic Habitat in Restored Riparian Sites of California's North Coast Rangelands. *Restoration Ecology*, *19*(2), 225-233.

Lewis, Q. W., & Rhoads, B. L. (2015). Rates and patterns of thermal mixing at a small stream confluence under variable incoming flow conditions. *Hydrological Processes*, *29*(20), 4442-4456.

Luce, C., Tonina, D., Gariglio, F., & Applebee, R. (2013). Solutions for the diurnally forced advection-diffusion equation to estimate bulk fluid velocity and diffusivity in streambeds from temperature time series. *Water Resources Research*, *49*, 488-506.

Luce, C. H., Tonina, D., Applebee, R., & DeWeese, T. (2017). Was that assumption necessary? Reconsidering boundary conditions for analytical solutions to estimate streambed fluxes. *Water Resources Research*, *53*(11), 9771-9790.

Malenda, H. F., Sutfin, N. A., Guryan, G., Stauffer, S., Rowland, J. C., Williams, K. H., & Singha, K. (2019). From Grain to Floodplain: Evaluating heterogeneity of floodplain hydrostatigraphy using sedimentology, geophysics, and remote sensing. *Earth Surface Processes and Landforms*, *44*(9), 1799-1815.

Marchand, J.-P., Biron, P., Buffin-Bélanger, T., & Larocque, M. (2022). High-resolution spatiotemporal analysis of hydrologic connectivity in the historical floodplain of straightened lowland agricultural streams. *River Research and Applications*, *38*(6), 1061-1079.

Marzadri, A., Tonina, D., Bellin, A. & Valli, A. Mixing interfaces, fluxes, residence times and redox conditions of the hyporheic zones induced by dune-like bedforms and ambient groundwater flow. *Advances in Water Resources*, 88, 139–151 (2016).

Menichino, G. T., & Hester, E. T. (2014). Hydraulic and thermal effects of in-stream structure-induced hyporheic exchange across a range of hydraulic conductivities. *Water Resources Research*, *50*(6), 4643-4661.

Merriam, E. R., & Petty, J. (2019). Stream channel restoration increases climate resiliency in a thermally vulnerable Appalachian river. *Restoration Ecology*, *27*(6), 1420-1428.

Monk, W. A., Wilbur, N. M., Allen Curry, R., Gagnon, R., & Faux, R. N. (2013). Linking landscape variables to cold water refugia in rivers. *Journal of Environmental Management*, *118*, 170-176.

Newman, B., Wilcox, B., & Graham, R. (2004). Snowmelt-driven macropore flow and soil saturation in a semiarid forest. *Hydrological Processes*, *18*, 1035-1042.

Nowinski, J. D., Cardenas, M. B., & Lightbody, A. F. (2011). Evolution of hydraulic conductivity in the floodplain of a meandering river due to hyporheic transport of fine materials. *Geophysical Research Letters*, *38*(1).

Poole, G. C., Stanford, J. A., Running, S. W., & Frissell, C. A. (2006). Multiscale geomorphic drivers of groundwater flow paths: subsurface hydrologic dynamics and hyporheic habitat diversity. *Journal of the North American Benthological Society*, *25*(2), 288-303.

Read, T., Bour, O., Bense, V., Le Borgne, T., Goderniaux, P., Klepikova, M. V., Hochreutener, R., Lavenant, N., & Boschero, V. (2013). Characterizing groundwater flow and heat transport in fractured rock using fiber-optic distributed temperature sensing. *Geophysical Research Letters*, *40*(10), 2055-2059.

Reeder, W. J., Gariglio, F., Carnie, R., Tang, C., Isaak, D., Chen, Q., Yu, Z., McKean, J. A. & Tonina, D. Some (fish might) like it hot: Habitat quality and fish growth from past to future climates. *Science of The Total Environment*, 787, 147532 (2021).

Richter, A., & Kolmes, S. A. (2005). Maximum temperature limits for Chinook, coho, and chum salmon, and steelhead trout in the Pacific Northwest. *Reviews in Fisheries science*, *13*(1), 23-49.

Ritter, T. D., Zale, A. V., Grisak, G., & Lance, M. J. (2020). Groundwater upwelling regulates thermal hydrodynamics and salmonid movements during high-temperature events at a

montane tributary confluence. *Transactions of the American Fisheries Society*, *149*(5), 600-619.

Rutherford, J. C., Marsh, N. A., Davies, P. M., & Bunn, S. E. (2004). Effects of patchy shade on stream water temperature: how quickly do small streams heat and cool? *Marine and Freshwater Research*, *55*(8), 737-748.

Samadder, R. K., Kumar, S., & Gupta, R. P. (2011). Paleochannels and their potential for artificial groundwater recharge in the western Ganga plains. *Journal of Hydrology*, *400*(1), 154-164.

Sawyer, A. H., Bayani Cardenas, M., & Buttles, J. (2012). Hyporheic temperature dynamics and heat exchange near channel-spanning logs. *Water Resources Research*, *48*(1).

Sawyer, A. H., & Cardenas, M. B. (2012). Effect of experimental wood addition on hyporheic exchange and thermal dynamics in a losing meadow stream. *Water Resources Research*, *48*(10).

Schilling, O. S., Partington, D. J., Doherty, J., Kipfer, R., Hunkeler, D., & Brunner, P. (2022). Buried Paleo-Channel Detection With a Groundwater Model, Tracer-Based Observations, and Spatially Varying, Preferred Anisotropy Pilot Point Calibration. *Geophysical Research Letters*, *49*(14).

Schmadel, N. M., Ward, A. S., Lowry, C. S., & Malzone, J. M. (2016). Hyporheic exchange controlled by dynamic hydrologic boundary conditions. *Geophysical Research Letters*, *43*(9), 4408-4417.

Sigurdsson, B. D., Aradóttir, Á., & Strachan, I. (1998). Cover and canopy development of a newly established poplar plantation in south Iceland. *Icel. Agric. Sci*, *12*, 15-26.

Singh, H. V., Faulkner, B. R., Keeley, A. A., Freudenthal, J., & Forshay, K. J. (2018). Floodplain restoration increases hyporheic flow in the Yakima River Watershed, Washington. *Ecological engineering*, *116*, 110-120.

Spanjer, A. R., Gendaszek, A. S., Wulfkuhle, E. J., Black, R. W., & Jaeger, K. L. (2022). Assessing climate change impacts on Pacific salmon and trout using bioenergetics and spatiotemporal explicit river temperature predictions under varying riparian conditions. *PLOS ONE*, *17*(5), e0266871.

Steiger, J., Tabacchi, E., Dufour, S., Corenblit, D., & Peiry, J.-L. (2005). Hydrogeomorphic processes affecting riparian habitat within alluvial channel–floodplain river systems: a review for the temperate zone. *River Research and Applications*, *21*(7), 719-737.

Sullivan, C. J., Vokoun, J. C., Helton, A. M., Briggs, M. A., & Kurylyk, B. L. (2021). An ecohydrological typology for thermal refuges in streams and rivers. *Ecohydrology*, *14*(5), e2295.

Tate, K. W., Lancaster, D. L., & Lile, D. F. (2007). Assessment of thermal stratification within stream pools as a mechanism to provide refugia for native trout in hot, arid rangelands. *Environmental Monitoring and Assessment*, *124*(1), 289-300.

Theodoropoulos, C., Stamou, A., Vardakas, L., Papadaki, C., Dimitriou, E., Skoulikidis, N., & Kalogianni, E. (2020). River restoration is prone to failure unless pre-optimized within a mechanistic ecological framework| Insights from a model-based case study. *Water Research*, *173*, 115550.

Tonina, D., & Buffington, J. M. (2009). Hyporheic exchange in mountain rivers I: Mechanics and environmental effects. *Geography Compass*, *3*(3), 1063-1086.

Tonina, D. & Buffington, J. M. Physical and biogeochemical processes of hyporheic exchange in alluvial rivers. *Groundwater Ecology and Evolution*, 61–87 (2023)

Torgersen, C. E., Ebersole, J. L., & Keenan, D. M. (2012). *Primer for identifying cold-water refuges to protect and restore thermal diversity in riverine landscapes* [Report].

Torgersen, C. E., Faux, R. N., McIntosh, B. A., Poage, N. J., & Norton, D. J. (2001). Airborne thermal remote sensing for water temperature assessment in rivers and streams. *Remote Sensing of Environment*, *76*(3), 386-398.

Torgersen, C. E., Price, D. M., Li, H. W., & McIntosh, B. A. (1999). MULTISCALE THERMAL REFUGIA AND STREAM HABITAT ASSOCIATIONS OF CHINOOK SALMON IN NORTHEASTERN OREGON. *Ecological Applications*, *9*(1), 301-319.

Tranmer, A. W., Caamaño, D., Clayton, S. R., Giglou, A. N., Goodwin, P., Buffington, J. M., & Tonina, D. (2022). Testing the effective-discharge paradigm in gravel-bed river restoration. *Geomorphology*, *403*, 108139.

Tranmer, A. W., Benjankar, R., & Tonina, D. (2020). Post-wildfire riparian forest recovery processes along a regulated river corridor. *Forest Ecology and Management*, *478*, 118513.

Tranmer, A. W., Marti, C. L., Tonina, D., Benjankar, R., Weigel, D., Vilhena, L., McGrath, C., Goodwin, P., Tiedemann, M., & Mckean, J. (2018). A hierarchical modelling framework for assessing physical and biochemical characteristics of a regulated river. *Ecological Modelling*, *368*, 78-93.

Tranmer, A. W., Weigel, D., Marti, C. L., Vidergar, D., Benjankar, R., Tonina, D., Goodwin, P., & Imberger, J. (2020). Coupled reservoir-river systems: Lessons from an integrated aquatic ecosystem assessment. *Journal of Environmental Management*, *260*, 110107.

U.S. Bureau of reclamation. (2018). *Grande Ronde River Numerical Hydraulic Modeling Study – Bird Track Springs Project Area* (Report SRH-2018-30)

U.S. Bureau of reclamation. (2016). *Groundwater evaluation and monitoring plan-Bird Track Springs Project Area* (Project E113000603)

van Kampen, R., Schneidewind, U., Anibas, C., Bertagnoli, A., Tonina, D., Vandersteen, G., Luce, C., Krause, S., & Van Berkel, M. (2022). *LPMLEn–A frequency domain method to estimate vertical streambed fluxes and sediment thermal properties in semi-infinite and bounded domains* (0043-1397).

Vinson, M. R. (2001). Long-term dynamics of an invertebrate assemblage downstream from a large dam. *Ecological Applications*, *11*(3), 711-730.

Weigel, D., Vilhena, L., Woods, P., Tonina, D., Tranmer, A., Benjankar, R., Marti, C., & Goodwin, P. (2017). Aquatic habitat response to climate-driven hydrologic regimes and water operations in a montane reservoir in the Pacific Northwest, USA. *Aquatic Sciences*, *79*, 953-966.

Westhoff, J. T., Paukert, C., Ettinger-Dietzel, S., Dodd, H., & Siepker, M. (2016). Behavioural thermoregulation and bioenergetics of riverine smallmouth bass associated with ambient cold-period thermal refuge. *Ecology of Freshwater Fish*, *25*(1), 72-85.

Wohl, E., Lane, S. N., & Wilcox, A. C. (2015). The science and practice of river restoration. *Water Resources Research*, *51*(8), 5974-5997.

Yuan, S.-y., Xu, L., Tang, H.-w., Xiao, Y., & Gualtieri, C. (2022). The dynamics of river confluences and their effects on the ecology of aquatic environment: A review. *Journal of Hydrodynamics*, *34*(1), 1-14.

Figures and Tables

Figure 1: Site Area

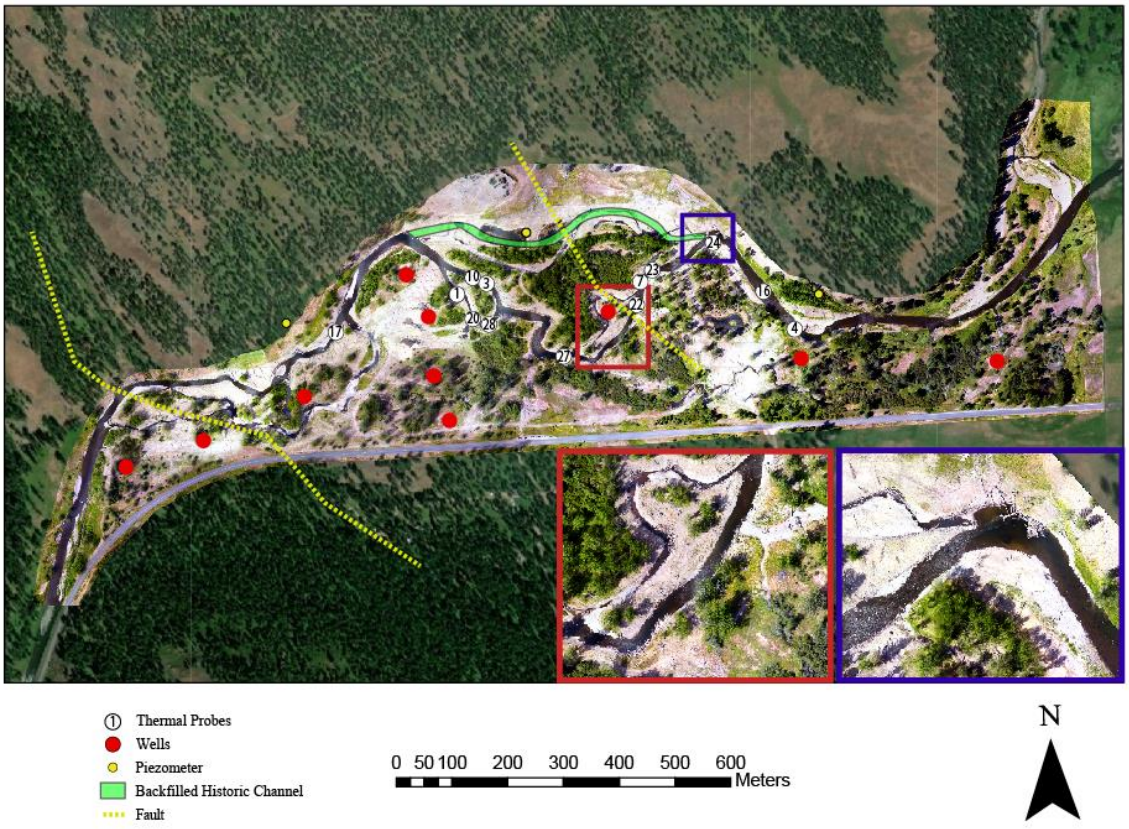

Figure 2: Water Temperatures for 2021 Water Year + GW Levels and Stage

- Figure 2a. Average daily gage height vs groundwater level
- Figure 2b. Average daily surface water and groundwater temperatures

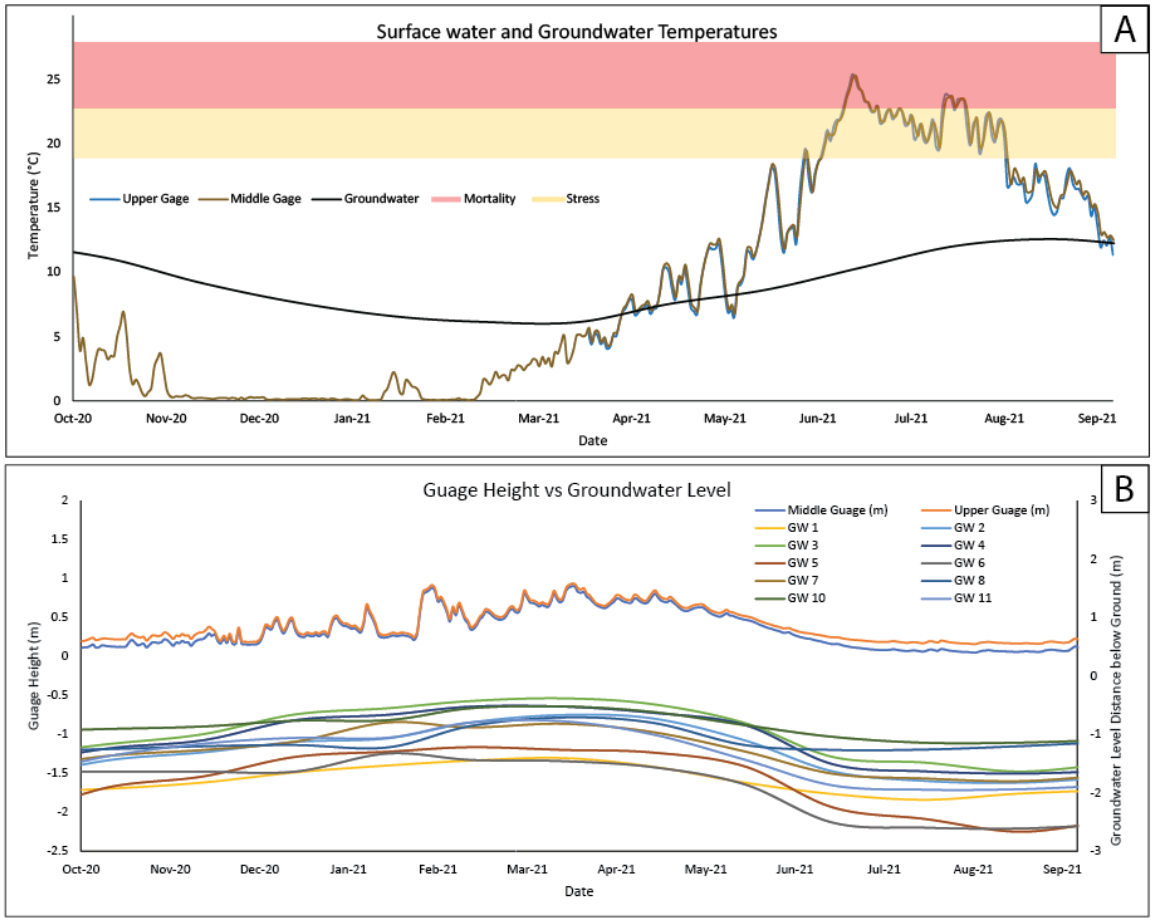

Figure 3: Valley Scale GW-SW Analysis With Discharge Measurement

- Valley scale SW-GW gradients coupled with discharge survey measurements

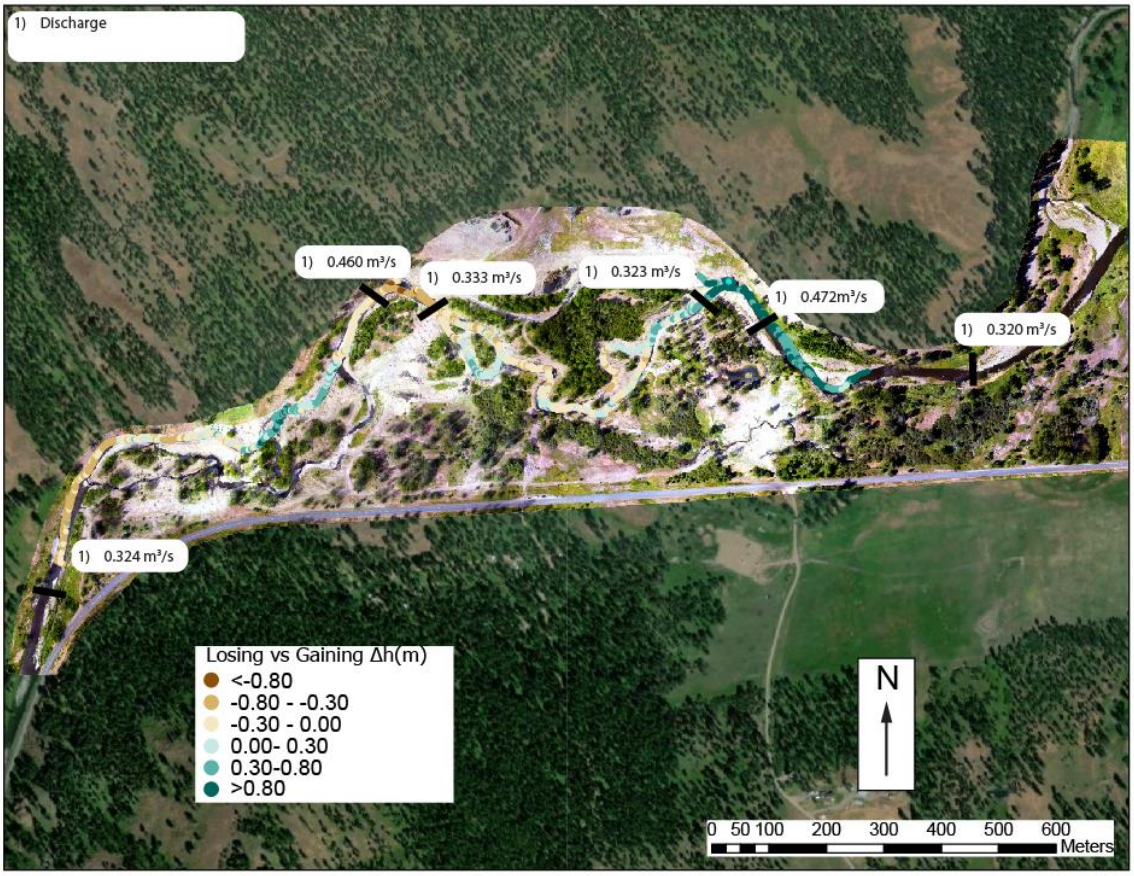

Figure 4: Box Plots for Each Morphology

- Box plots for each morphologic feature derived from thermal survey

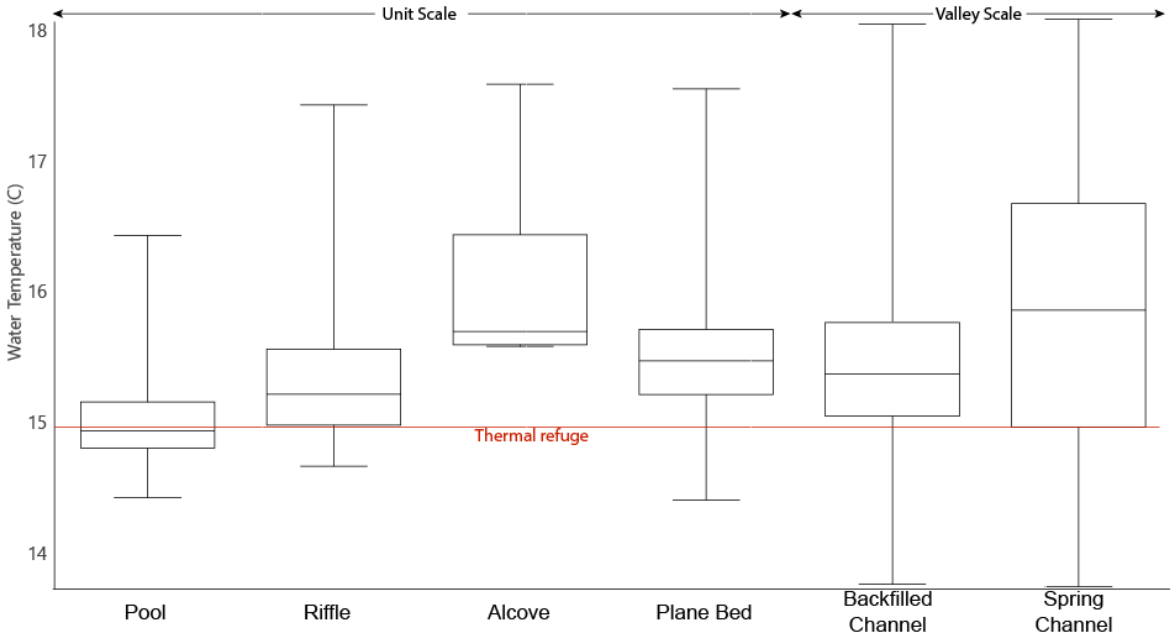

Figure 5: Spring Channels

- Water temperature signal in spring channels during thermal survey. Same locations as cutouts from figure 1

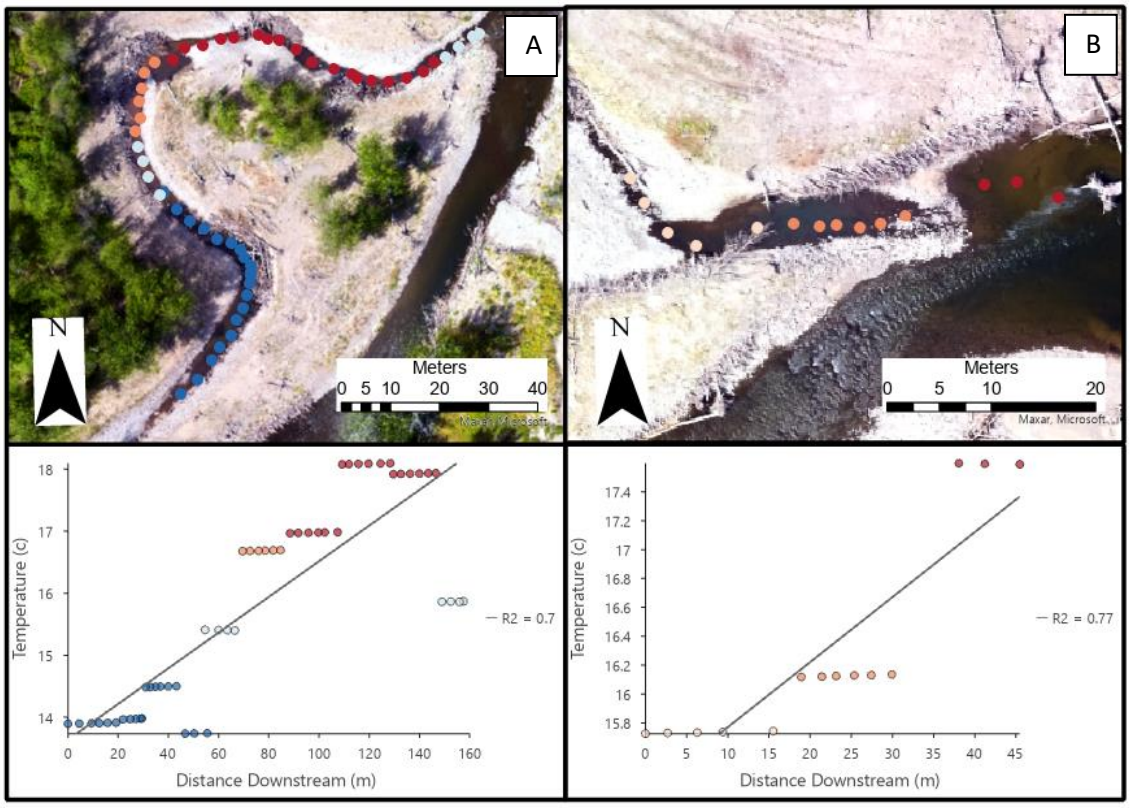

Figure 6: Temperatures at Exit of Backfilled Channel

- Same location as figure 5b
- This figure shows the complex mixing mechanism at this pool. SW from the spring channel and subsurface hyporheic from the backfilled channel converge here

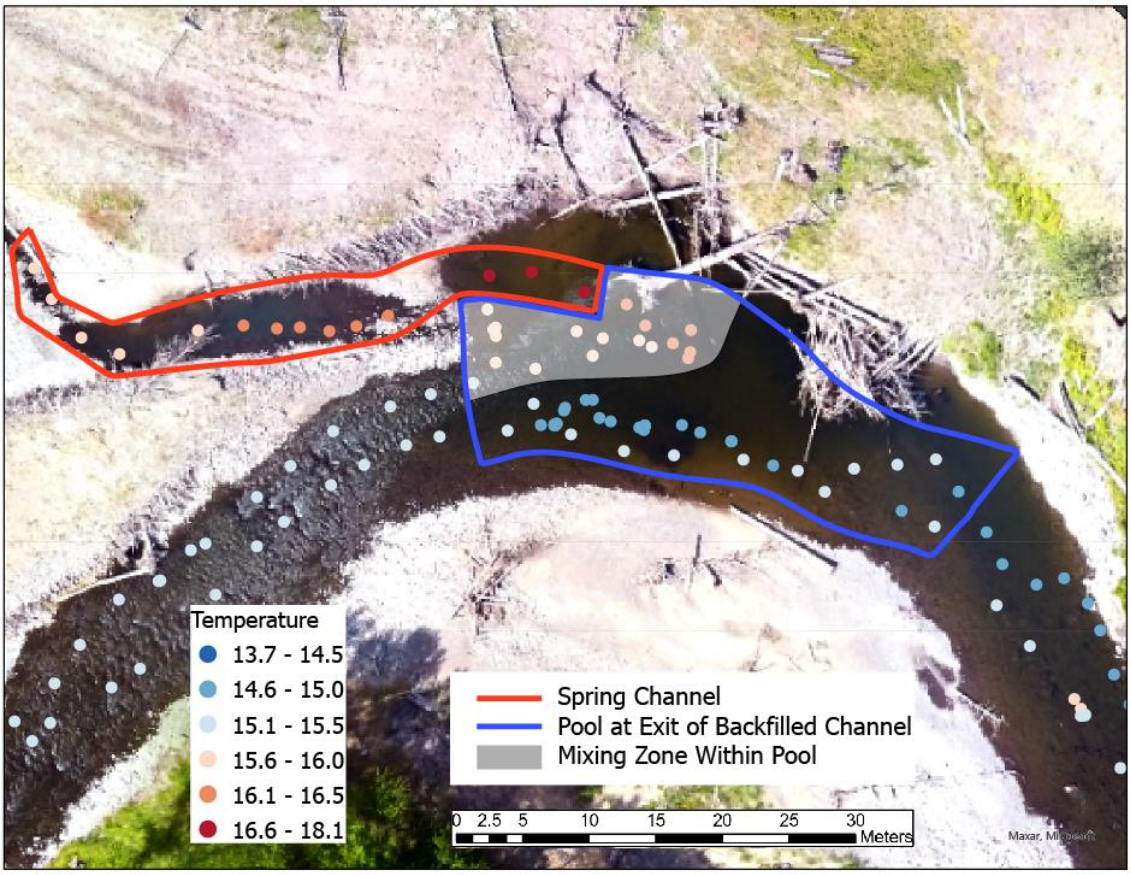

Table 1: Can Unit-scale Features Overwhelm Groundwater Gradients

- Chart compares agreement between flux direction reported in the probes and the direction of the valley scale groundwater gradient to determine whether localized flux from unit scale features are capable of overwhelming the valley-scale groundwater gradients. Morphological units are abbreviated as: RT-Riffle Tail, PT-Pool Tail, PM-Pool Middle, PH-Pool Head, S-Spring Channel, PB-Plane Bed. N/A in the "Local Hyporheic overwhelming Valley-scale Hyporheic" column means the expected effect of the morphologic unit is in agreement with the valley scale groundwater gradients, therefore we are not able to evaluate whether the morphologic unit is capable of overwhelming the valley scale gradients.

Probe #	Hyporheic Flux Probe (U/D)	Valley-scale Groundwater Gradient (U/D)	Probe vs Valley-scale Match?	Morphology Unit	Expected Effect of Morphology Unit	Local Hyporheic overwhelming Valley-scale Hyporheic
3	Down	Down	Yes	RT	Up	No
4	Up	Up	Yes	PH	Up	N/A
7	Up	Up	Yes	RT	Up	N/A
16	Up	Up	Yes	PB	None	N/A
17	Up	Up	Yes	PT	Down	No
20	Up	Up	Yes	PH	Up	N/A
21	Up	Up	Yes	S	None	N/A
22	Up	Down	No	PB	None	N/A
23	Up	Up	Yes	PT	Down	No
27	Down	Down	Yes	PT	Down	N/A
28	Up	Up	Yes	PM	Down	No

Appendix A

Figure A1: GPS Unit Set up for Thermal Survey and Hyporheic Flux Probe Construction

Figure A2: Valley Scale GW-SW Analysis Methodology

- This image depicts the curved drawdown profile of the groundwater table as it approaches the stream. They valley-scale groundwater gradients omit this profile, a

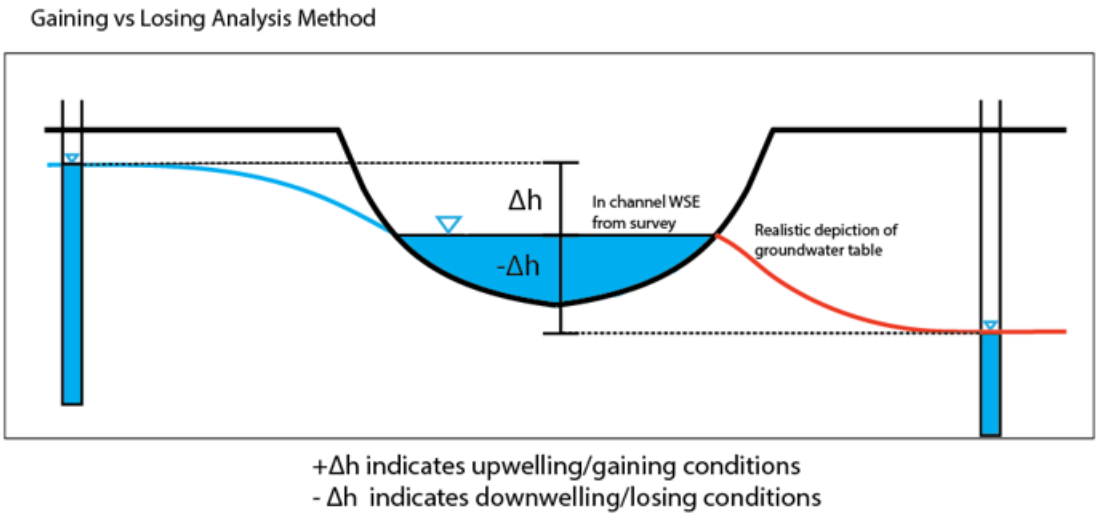

limitation of this analysis.

Figure A3: Mechanisms maintaining cool pool temperatures

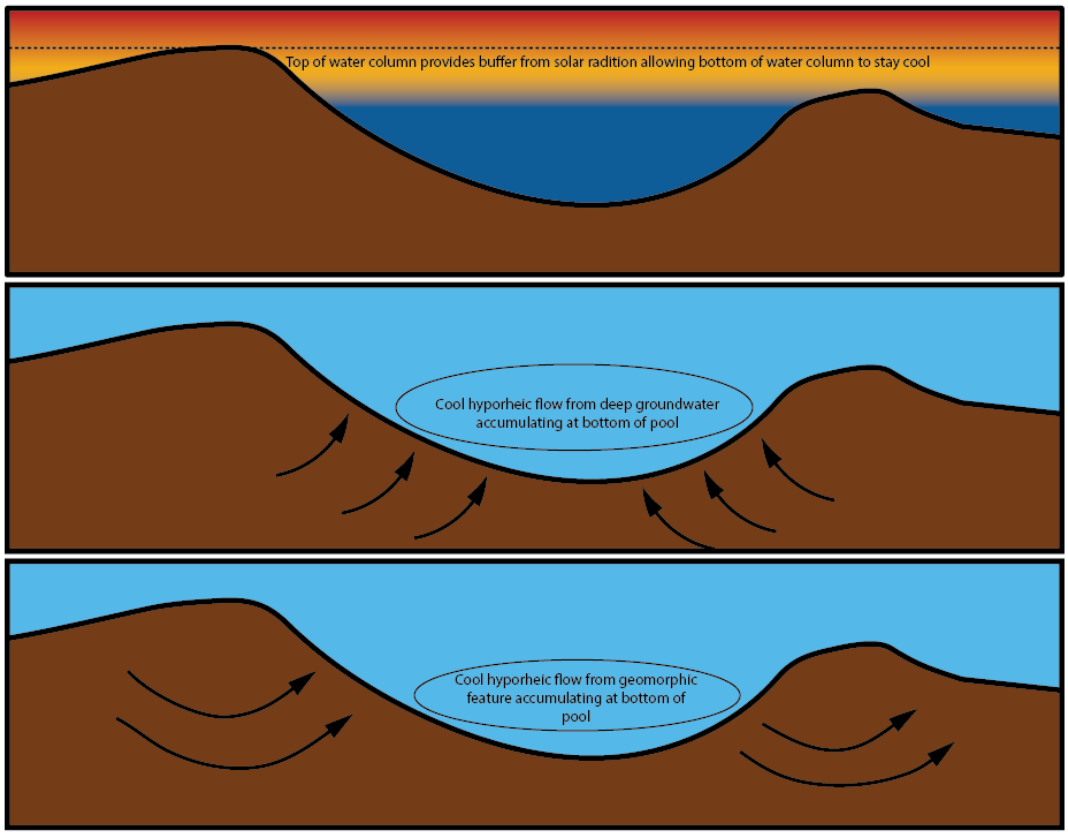

Figure A4: Fluxes of all probes

- Hyporheic flux probes calculated magnitude throughout the year

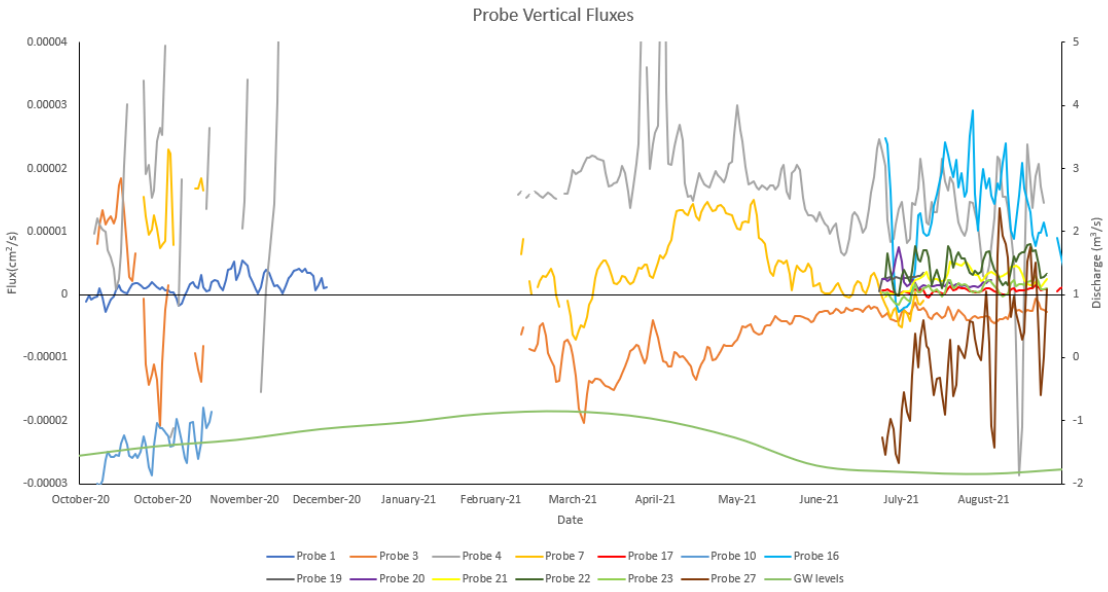

Figure A5: Fish Snorkel Survey

- Pool temperatures during snorkel survey. Ambient Temperature is the average temp of the feature and its immediate surroundings. Minimum temperature is the lowest temperature from the pool bottom.